HHS Public Access

Author manuscript

Eur J Inorg Chem. Author manuscript; available in PMC 2016 October 01.

Published in final edited form as:

Eur J Inorg Chem. 2015 October ; 2015(30): 5021–5026. doi:10.1002/ejic.201500816.

Synthesis and assessment of CO-release capacity of manganese carbonyl complexes derived from rigid α-diimine ligands of varied complexity

Jorge Jimenez, **Indranil Chakraborty**, and **Pradip K. Mascharak***

Contribution from the Department of Chemistry and Biochemistry, University of California, Santa Cruz, CA 95064, USA

Abstract

Four manganese carbonyl complexes of the type $[MnBr(CO)_3(N^N)]$ (N^N = α-diimine ligands) namely $[MnBr(CO)_3(bpy)]$ (**1**), $[MnBr(CO)_3(phen)]$ (**2**), $[MnBr(CO)_3(dafo)]$ (**3**) and $[MnBr(CO)_3(pyzphen)]$ (**4**) (where bpy = bipyridine, phen = 1,10-phenanthroline, dafo = 4,5-diazafluoren-9-one and pyzphen = pyrazino[2,3-f][1,10]-phenanthroline) have been synthesized and structurally characterized. These four complexes containing the *fac*-$[Mn(CO)_3]$ motif release CO upon illumination with low power visible and UV light. The CO release rates and the absorption maxima of the complexes are however very similar despite systematic increase in structural complexity in the rigid α–diimine ligand frames. This is quite in contrary to manganese carbonyl complexes derived from α–diimine ligands in which at least one of the imine functions is not part of the rigid ring systems. Results of this study will provide help in the future design of ligand frames suitable for the syntheses of photoCORMs to deliver CO to biological targets under the control of light.

Keywords

Manganese complexes; α-diimine ligands; CO photo release; metal carbonyl complexes

Introduction

The therapeutic potential of carbon monoxide (CO) has been realized relatively recently [1–3]. For long time, this diatomic molecule has been considered as highly toxic due to its ability to bind hemoglobin and effectively reducing the oxygen-carrying capacity of the blood, leading to hypoxia. Surprisingly during the past few years, controlled dosage of carbon monoxide has been shown to elicit salutary effects in mammalian physiology. In relatively low concentrations (>200 ppm) CO imparts anti-inflammatory, anti-apoptotic and vasoregulatory effects. More interestingly, moderately high concentration of CO exerts pro-apoptotic effects toward aggressive T cells, dysregulated hyperproliferative smooth muscle cells, and cancer cells [1,4,5]. Because of its toxic nature, use of gaseous CO is somewhat

pradip@ucsc.edu, Phone: (831) 459-4251, (Pradip K. Mascharak).

CCDC 977176 and 1413849 – 1413851 contain the supplementary crystallographic data for this paper. These data can be obtained free of charge from the Cambridge Crystallographic Data centre via http://www.ccdc.cam.ac.uk/data_request/cif.

prohibitive in hospital settings. The quest for suitable therapeutics (prodrugs) for delivering CO to biological targets under controlled conditions has therefore emerged as an area of considerable research interest [6–8].

Metal carbonyl complexes have been studied extensively for various purposes over the years due to their well-known photophysical and photochemical properties [9]. A detail understanding of such properties eventually established the potential of these complexes as CO releasing molecules (CORMs) to deliver CO in a more controlled fashion to biological targets compared to its gaseous form [10]. Moreover the photophysical and photochemical properties have been shown to be strongly dependent on nature of the ligands and co-ligands employed in the syntheses [9]. Based on such principles a new class of photo-induced carbon monoxide releasing molecules (photoCORMs) has been developed in the recent years where CO delivery could be triggered under the control of light [11–15].

Among others, the group 7 metal carbonyls of general formula $[MX(CO)_3(N^N)]$ (where, M = Mn, Re, X = Cl, Br, N^N = α-diimine ligand) have been most widely studied in terms of their spectroscopic properties [9]. Herein we chose to examine the relative light induced capacity of CO release of Mn(I) complexes derived from four different rigid bidentate α-diimine ligands. The complexes namely, $[MnBr(CO)_3(bpy)]$ (**1**), $[MnBr(CO)_3(phen)]$ (**2**), $[MnBr(CO)_3(dafo)]$ (**3**) and $[MnBr(CO)_3(pyzphen)]$ (**4**) (where bpy = bipyridine, phen = 1,10-phenanthroline, dafo = 4,5-diazafluoren-9-one and pyzphen = pyrazino[2,3-f] [1,10]phenanthroline) (Scheme 1) have been synthesized and characterized with the aid of various analytical techniques including X-ray crystallography. The αdiimine ligands have been chosen in such a way to systematically increase the complexity of the ligand frame. In going from bpy to phen there is an increase in π-conjugation. The complexity in the ligand frame is further increased in case of dafo through the introduction of the exocyclic keto group along with strained five-membered ring and in pyzphen through an additional pyrazine ring attached to the phen ligand moiety. Our goal was to examine the modulation of the M–CO bond labilization in this set of analogous manganese carbonyl complexes due to modifications in the α-diimine ligand frame. As reported in the following sections, complexes **1**–**4** surprisingly exhibit minimal changes in their parameters for CO photorelease despite significant alterations in the α-diimine ligand frame.

Results and Discussion

Complexes **1**–**4** have been isolated from the reaction of $[MnBr(CO)_5]$ with one equivalent of the appropriate α-diimine ligand (bpy, phen, dafo and pyzphen) in dichloromethane at room temperature. Yellow to orange crystals of these complexes are stable under ambient conditions for several months. Despite previous reports on spectroscopic properties of **1** and **2**, no structural information on this set of analogous manganese carbonyl complexes was available.

We have therefore determined the structures of all four complexes and carefully examined their metric features before determining their CO releasing properties. The molecular structures of the complexes are shown in Figures 1–4 and the crystallographic data are listed in Table 1. Although the complexes are isostructural, close inspection of their structural

parameters reveals subtle differences. As shown in Figures 1–4, the Mn(I) center in all four complexes reside in a distorted octahedral geometry. The equatorial plane consists of two N atoms from the bidentate ligands and two C atoms of the CO groups while the third CO and the bromide ligand occupy the axial positions. As a consequence, all four complexes comprise the *fac*-[$Mn(CO)_3$] motif.

The equatorial planes for complexes **1** and **3** are satisfactorily planar with mean deviations of 0.016 and 0.039 Å respectively. In case of **2** and **4** the equatorial atoms constitute a perfect plane. The five-membered chelate rings for **1** and **3** exhibit minimal deviation from the planarity (mean deviations of 0.006 Å in **1** and 0.005 Å in **3**) compared to that noted in **3** and **4** (mean deviation 0.030 and 0.028 Å respectively). Average Mn–N distances in complexes **1**, **2** and **4** are very similar (2.043(3), 2.052(2) and 2.055(2) Å respectively) in contrast to the average Mn–N distance in complex **3** (2.119(6) Å). This relatively longer average Mn–N bond length of **3** is consistent with larger bite distance of the two coordinating N atoms of dafo ligand compared to that of bpy, phen and pyzphen in their respective complexes.

The *fac*-[$Mn(CO)_3$] moiety of complexes **1**–**4** also shows some variations. For example, the Mn–CO(axial) distances in **2**, **3** and **4** are consistently longer (1.858(4), 1.911(10) and 1.867(6) Å respectively) compared to the average of the respective Mn–CO(equatorial) distances (1.806(3)–1.811(4) Å range). In case of **1**, the Mn–CO(axial) and the average of Mn-CO(equatorial) distances are however comparable. Finally, the Mn–Br bond lengths (span the range 2.510–2.544 Å) in the present complexes are similar to those noted for other manganese carbonyl complexes with bidentate ligands [16–18].

The facial disposition of the three CO ligands in **1**–**4** is readily evident from two strong ν_{CO} stretching bands around 1920 and 2030 cm^{-1} in their FTIR spectra. All four complexes exhibit ^1H NMR spectra consistent with the diamagnetic ground state for the Mn(I) centers (low spin t_{2g}^6 configuration). The complexes are fairly soluble in solvents like chloroform and dichloromethane. Solutions of **1**–**4** in dichloromethane are stable for long period of time in absence of light as monitored by spectrophotometry. The electronic absorption spectra of the complexes in such solvent consist of two bands (Figure 5). The broad absorption band in the range of 500–350 nm can be attributed to the metal-to-ligand charge transfer (MLCT) transitions with contribution from bromide-to-metal charge transfer (XLCT) [9, 12].

Complexes **1**–**4** readily release CO upon exposure to *low power visible light* (15 mW/cm^2). The systematic decrease of MLCT band upon such illumination was indicative of CO photorelease from the respective complexes (as also corroborated with reduced myoglobin assay). One representative case of UV-Vis spectral changes due to visible light induced CO release from complex **3** is shown in Figure 6.

In dichloromethane solutions the complexes, **1**, **2**, **3** and **4** exhibited the apparent CO release rate (k_{CO}) of 1.21 ± 0.02, 4.65 ± 0.03, 3.44 ± 0.02, and 6.29 ± 0.03 min^{-1} respectively (Table 2). The k_{CO} values clearly indicate that in all these complexes, the added conjugation and/or heteroatoms in the ligand frames do not impart significant advantages in terms of their ease of CO release. The trend is similar when the k_{CO} were measured under low power

(3 mW/cm^2) UV illumination (Table 2). This finding is in contrary to that observed for metal carbonyl complexes derived from non-rigid α-diimine frames shown in Scheme 2. With manganese carbonyl complexes derived from these ligands, both red shift and enhanced light absorption were evident upon *increase in conjugation* or *introduction of heteroatoms* within the ligand frame. The former modification stabilized the lowest unoccupied orbitals whereas the later contributed towards destabilization of the highest occupied orbitals [12]. Thus, the MLCT maximum of [MnBr(CO)$_3$(pmtpm)] shifts from 500 nm to 535 nm in case of [MnBr(CO)$_3$(qmtpm)] upon replacement of the pyridine ring with quinoline. Similarly, [Mn(MeCN)(CO)$_3$(qmtpm)] exhibits a higher k_{CO} value ((2.0 ± 0.01) × 10^{-3} s^{-1}) compared to [Mn(MeCN)(CO)$_3$(pimq)] (k_{CO} = (0.13 ± 0.01) × 10^{-3} s^{-1}) due to the presence of the –SMe appendage. Quite in contrast, for the present manganese complexes derived from rigid α-diimine ligands no striking difference in apparent CO release rates have been noticed upon such alterations. It is also important to note that such alterations do not cause shift in the MLCT band maxima of these complexes (Figure 5). In addition, cyclic voltammetry studies reveal no significant differences in E_{pa} (anodic potential) values for the Mn(I) to Mn(II) oxidation (Table 3), an observation consistent with the similar MLCT band maxima of **1**–**4**.

The nature of photoproducts of the complexes has been closely examined in the present study. Following exhaustive photolysis of acetonitrile solutions with the aid of visible light, X-band EPR spectra of the photoproducts were recorded. The distinct 6 line EPR spectra indicated the presence of Mn(II) (I = 5/2) in such solutions. One representative spectrum is shown in Figure 7 (top panel). The solids obtained upon complete evaporation of the bulk solution in the photolysis experiments were also subjected to solid-state IR study. In KBr matrix the IR spectra exhibited no CO stretch, a pattern consistent with some of our previous reports [17, 18]. Because the ligands employed in the present work are all fluorescent, any loss of ligands from the photoproducts is expected to display luminescence. Luminescence studies with the photolyzed solutions however exhibited no fluorescence associated with CO release from **1**–**4**. Taken together, these results indicated that upon illumination, all three coordinated CO molecules are released from **1**–**4** and the α-diimine ligands remain coordinated to the Mn(II) centers in the respective photoproducts along with solvent molecules e.g. MeCN. This assignment is further corroborated by the X-band EPR spectrum of a reaction mixture of Mn(ClO$_4$)$_2$, 1,10-phenanthroline, and (Et$_4$N)Br (1:1:1) in acetonitrile (Figure 7, bottom panel). The similarities between the two spectra strongly suggest that exhaustive photolysis of complexes **1**–**4** leads to [MnBr(N^N)(solv)$_3$]$^+$ (N^N = α-diimine ligands) as the final photoproducts in solution under aerobic conditions.

Conclusions

In summary, the results of this study clearly demonstrate that in four manganese carbonyl complexes with [Mn(CO)$_3$] motif, incorporation of rigid α–diimime ligands with increasing complexity in terms of additional conjugation and heteroatoms does not lead to striking differences in their capacity of CO photorelease. In addition, such alterations result in small shifts in their MLCT band maxima and Mn(I)/Mn(II) redox potentials. These findings are quite in contrary to that noted in other manganese carbonyl complexes with of α-diimine ligands in which at least one of the imine functions is not a part of rigid ring systems [12].

We anticipate that these observations will serve as useful guidelines for designing future ligands for photoCORMs suitable for CO release upon exposure to visible light (desired in phototherapy).

Experimental Section

Materials and Methods

$[Mn(CO)_5Br]$ was purchased from Strem Chemicals. Bipyridine, 1,10-phenanthroline, pyrazino[2,3-f][1,10]phenanthroline, and horse heart myoglobin (Mb) were purchased from Sigma-Aldrich and used as received. The solvents were purified according to the standard procedures [19]. 4,5-Diazafluoren-9-one was synthesized following a reported procedure [20]. Synthesis of $[MnBr(CO)_3(bpy)]$ (**1**) was completed by following a procedure previously reported by us [21].

UV-Vis spectra were obtained with Varian Cary 50 UV-Vis spectrophotometer. A Perkin-Elmer Spectrum-One FT IR spectrometer was employed to monitor the IR spectra of the reported compounds. X-band EPR spectra were recorded at 120 K using a Bruker 500 ELEXSYS spectrometer. Microanalyses were carried out with a Perkin Elmer Series II elemental analyzer. A BASi-EPSILON electrochemistry system was employed in the cyclic voltammetry studies. Tetrabutylammonium hexaflurophosphate ($TBAPF_6$) was used as the supporting electrolyte.

$[MnBr(CO)_3(phen)]$ (2)

A slurry of 80 mg (0.29 mmol) of $[Mn(CO)_5Br]$ and 53 mg (0.30 mmol) of 1,10-phenantroline in 18 mL of dichloromethane was stirred for 20 h at RT when the color of the solution turned orange. The volume of the solvent was reduced under vacuum and a yellow powder was obtained upon addition of diethyl ether and subsequent cooling at 5 °C. The solid thus obtained was filtered and washed with dichloromethane. Yield (61 mg, 53% yield). Anal. Cal. for $C_{15}H_8BrN_2O_3Mn$: C, 45.14; H, 2.02; N, 7.02%. Found: C, 45.21; H, 1.98; N, 7.08%. Selected IR (KBr, cm^{-1}): ν_{CO} 2021 and 1941. UV-Vis spectrum in dichloromethane solution, λ_{max} (nm) [ε (M^{-1} cm^{-1})]: 430 (3 770), 380 (3 680), 270 (41 150).

$[MnBr(CO)_3(dafo)]$ (3)

A slurry of 100 mg (0.36 mmol) of $[Mn(CO)_5Br]$ and 73 mg (0.40 mmol) of 4,5-diazafluoren-9-one in 25 mL of dichloromethane was allowed to stir at RT for 20 h. The solution turned red during this time. A dark orange powder was obtained upon evaporation of this solution under reduced pressure. The solid was recrystallized by layering hexanes over a solution of the complex in dichloromethane. Yield (90 mg, 62.5%). Anal. Cal. for $C_{14}H_6BrN_2O_4Mn$: C, 41.93; H, 1.51; N, 6.98%. Found: C, 42.10; H, 1.59; N, 7.01%. Selected IR (KBr, cm^{-1}): ν_{CO} 2030 and 1926. UV-Vis spectrum in dichloromethane solution, λ_{max} (nm) [ε (M^{-1} cm^{-1})]: 430 (2 370), 300 (10 450).

[MnBr(CO)$_3$(pyzphen)] (4)

A slurry of 80 mg (0.29 mmol) of [Mn(CO)$_5$Br] and 70 mg (0.30 mmol) of pyrazino[2,3-f][1,10]phenanthroline in 30 mL of dichloromethane was allowed to stir at RT for 18 h. The solvent was then removed under reduced pressure and the orange powder was recrystallized from dichloromethane. Yield (104 mg, 80 % yield). Anal. Cal. for $C_{17}H_8BrN_4O_3Mn$: C, 45.26; H, 1.78; N, 12.42%. Found: C, 45.32; H, 1.80; N, 12.31%. Selected IR (KBr, cm^{-1}): ν_{CO} 2026 and 1925. UV-Vis spectrum in dichloromethane solution, λ_{max} (nm) [ε (M^{-1} cm^{-1})]: 430 (2 350), 260 (37 600).

X-ray data collection and structure refinement

Orange crystals of [MnBr(CO)$_3$(bpy)] (**1**) and [MnBr(CO)$_3$(dafo)] (**3**) were obtained by layering hexanes over their dichloromethane solutions while slow evaporation of dichloromethane solutions afforded yellow crystals of [MnBr(CO)$_3$(phen)] (**2**) and [MnBr(CO)$_3$(pyzphen)] (**4**). Data were collected on Bruker APEX II single crystal X-ray diffractometer with graphite monochromated Mo Kα radiation (λ = 0.71073 A) by ω-scan technique in the range of $3 \leq 2\theta \leq 49$ for **1**, $3 \leq 2\theta \leq 48$ for **2**, $3 \leq 2\theta \leq 49$ for **3** and $3 \leq 2\theta \leq 48$ for **4**. All data were corrected for Lorentz-polarization and absorption [22]. The metal atoms were located from Patterson maps and the rest of the non-hydrogen atoms emerged from successive Fourier syntheses. The structures were refined by a full-matrix least squares procedure on F^2. All the non-hydrogen atoms were refined anisotropically and the hydrogen atoms were included in calculated positions. Absorption corrections were performed using SADABS. Structures were solved by using the SHELXTL™ V6.14 program package [23].

Photolysis experiment

The rates of CO release upon exposure to visible and UV light were measured with solutions of the complexes in 1 × 0.4 cm quartz cuvette. The light source employed in this study included an IL-410 illumination system (Electro FiberOptics Corporation; power, 15 mW/cm^2) and a UV transilluminator model LM-20 (UVP Inc.; power, 3 mW/cm^2). The cuvette was placed at a distance of 1 cm from the light source. Prior to recording each spectrum, the cuvette was inverted homogenously to ensure proper mixing. Apparent CO release was followed at an appropriate wavelength for each complex and the logarithm of complex concentration versus time plots were obtained. Horse heart myoglobin was dissolved on phosphate buffer saline (PBS, 100 mM, pH 7.4) and reduced by adding sodium dithionite. Because sodium dithionite is known to facilitate the release of CO [24], an apparatus was constructed using two quartz cuvettes. In the first cuvette under anaerobic conditions, the photoactive complex was exposed to the visible light evolving CO into the headspace. The photo released CO was then transferred into the second cuvette containing the reduced Mb solution under a positive N_2 pressure.

Acknowledgments

Financial support from National Science Foundation Grant DMR-1409335 is gratefully acknowledged. JJ was supported by the NIH grant 2R25GM058903. We thank Dr. Logesh Mathivathanan and Graham Roseman for help in electrochemistry and EPR measurements.

References

1. Motterlini R, Otterbein LE. Nat Rev Drug Discovery. 2010; 9:728–743. [PubMed: 20811383]
2. Kim HP, Ryter SW, Choi AMK. Ann Rev Pharmacol Toxicol. 2006; 46:411–449. [PubMed: 16402911]
3. Ryter SW, Choi AMK. Korean J Intern Med. 2013; 28:123–140. [PubMed: 23525151]
4. McDaid J, Yamashita K, Chora A, Ilinger R, Strom TB, Li XC, Bach FH, Soares MP. FASEB J. 2005; 19:458–460. [PubMed: 15640283]
5. Song R, Zhou Z, Kim PKM, Shapiro RA, Liu F, Ferran C, Choi AMK, Otterbein LE. J Biol Chem. 2004; 279:44327–44334. [PubMed: 15280387]
6. Mann BE, Motterlini R. Chem Commun. 2007:4197–4208.
7. Alberto R, Motterlini R. Dalton Trans. 2007:1651–1660. [PubMed: 17443255]
8. Johnson TR, Mann BE, Clark JE, Foresti R, Green CJ, Motterlini R. Angew Chem Int Ed. 2003; 42:3722–3729.
9. Stufkens DJ, Vlcek A Jr. Coord Chem Rev. 1998; 177:127–179.
10. Romao CC, Blattler WA, Seixas JD, Bernardes GDL. Chem Soc Rev. 2012; 41:3571–3583. [PubMed: 22349541]
11. Schatzschneider U. Brit J Pharmacol. 2015; 172:1638–1650. [PubMed: 24628281]
12. Chakraborty I, Carrington SJ, Mascharak PK. Acc Chem Res. 2014; 47:2603–2611. [PubMed: 25003608]
13. Heilman BJ, Gonzalez MA, Mascharak PK. Prog Inorg Chem. 2014; 58:185–224.
14. Rimmer RD, Pierri AE, Ford PC. Coord Chem Rev. 2012; 256:1509–1519.
15. Schatzschneider U. Inorg Chim Acta. 2011; 374:19–23.
16. Carrington SJ, Chakraborty I, Mascharak PK. Chem Commun. 2013; 49:11254–11256.
17. Carrington SJ, Chakraborty I, Bernard JML, Mascharak PK. ACS Med Chem Lett. 2014; 5:1324–1328. [PubMed: 25516792]
18. Carrington SJ, Chakraborty I, Mascharak PK. Dalton Trans. 2015; 44:13828–13834. [PubMed: 25952559]
19. Perrin, DD.; Armarego, WLF. Purification of Laboratory Chemicals. Pergamon Press; 1988.
20. Eckhard IF, Summers LA. Aust J Chem. 1973; 26:2727–2728.
21. Chakraborty I, Carrington SJ, Mascharak PK. ChemMedChem. 2014; 9:1266–1274. [PubMed: 24756950]
22. North ACT, Philips DC, Mathews FS. Acta Crystallogr, Sect C. 1968; 24:348–351.
23. Sheldrick, GM. SHELXTL™ V 6.14. Bruker Analytical X-ray Systems. Madison, WI: 2000.
24. McLean S, Mann BE, Poole RK. Anal Biochem. 2012; 427:36–40. [PubMed: 22561917]

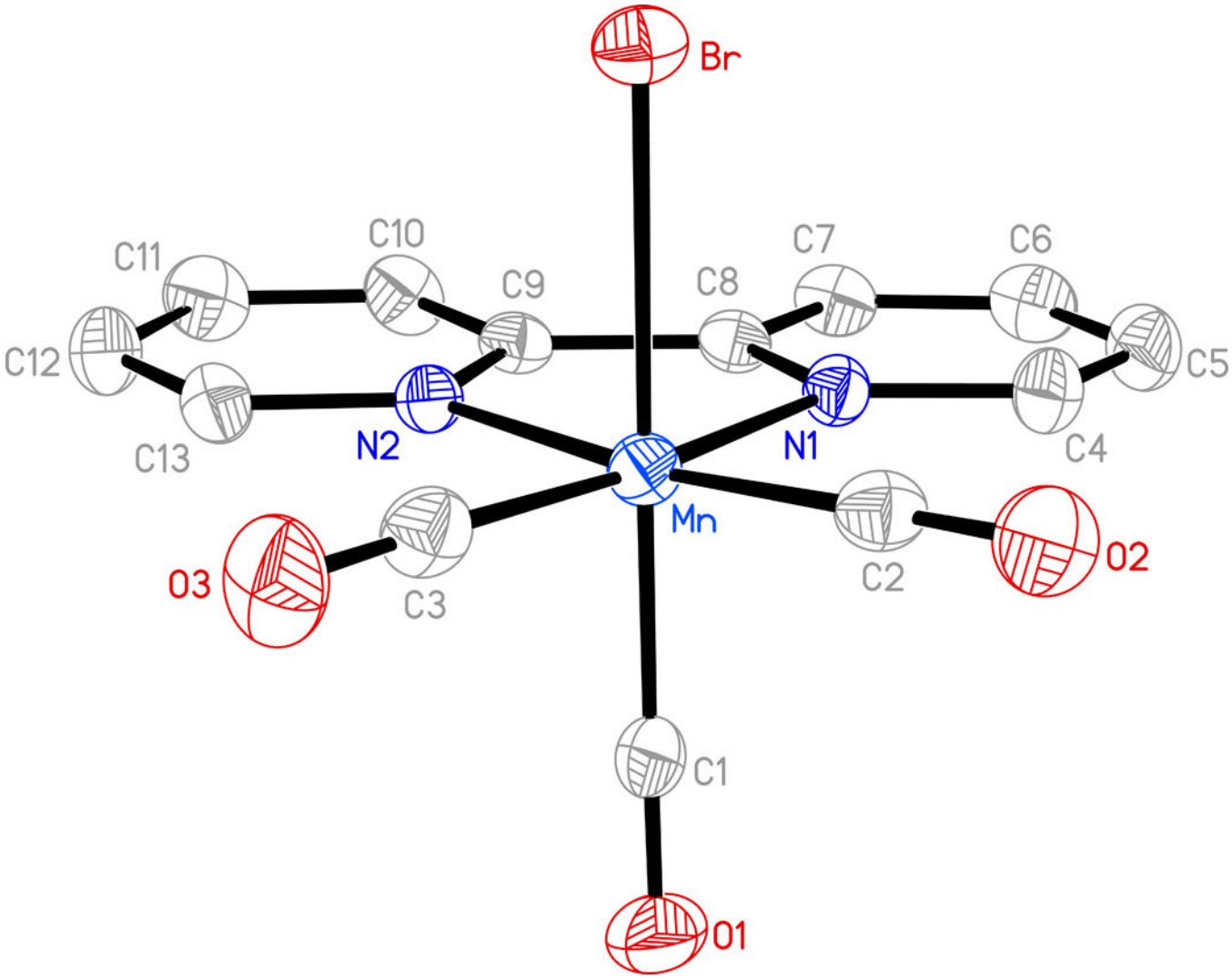

Figure 1.

Molecular structure of $[MnBr(CO)_3(bpy)]$ (**1**) (thermal ellipsoids are shown at 50% probability level and the hydrogen atoms are omitted for clarity) and selected bond distances (Å): Molecule A: Mn-C(1) 1.803(4), Mn-C(2) 1.809(4), Mn-C(3) 1.814(4), Mn-N(1) 2.043(3), Mn-N(2) 2.052(2), Mn-Br 2.5316(11). Molecule B: Mn(1)-C(14) 1.800(4), Mn(1)-C(15) 1.799(4), Mn(1)-C(16) 1.790(4), Mn(1)-N(3) 2.041(3), Mn(1)-N(4) 2.035(3), Mn(1)-Br(1) 2.5441(11).

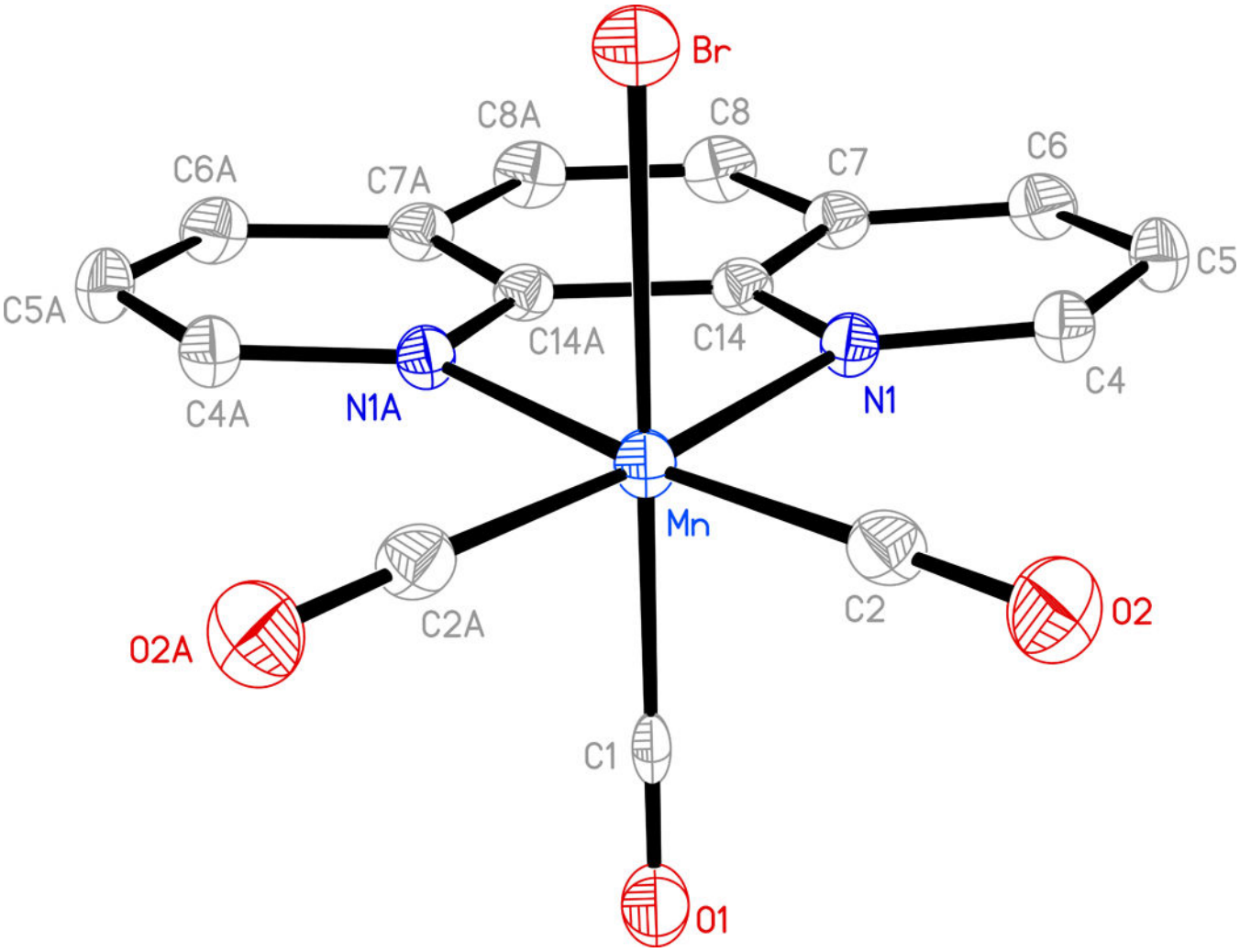

Figure 2.

Molecular structure of $[MnBr(CO)_3(phen)]$ (**2**) (thermal ellipsoids are shown at 50% probability level and the hydrogen atoms are omitted for clarity) and selected bond distances (Å): Mn-C(1) 1.858(4), Mn-C(2) 1.806(3), Mn-Br 2.5249(7).

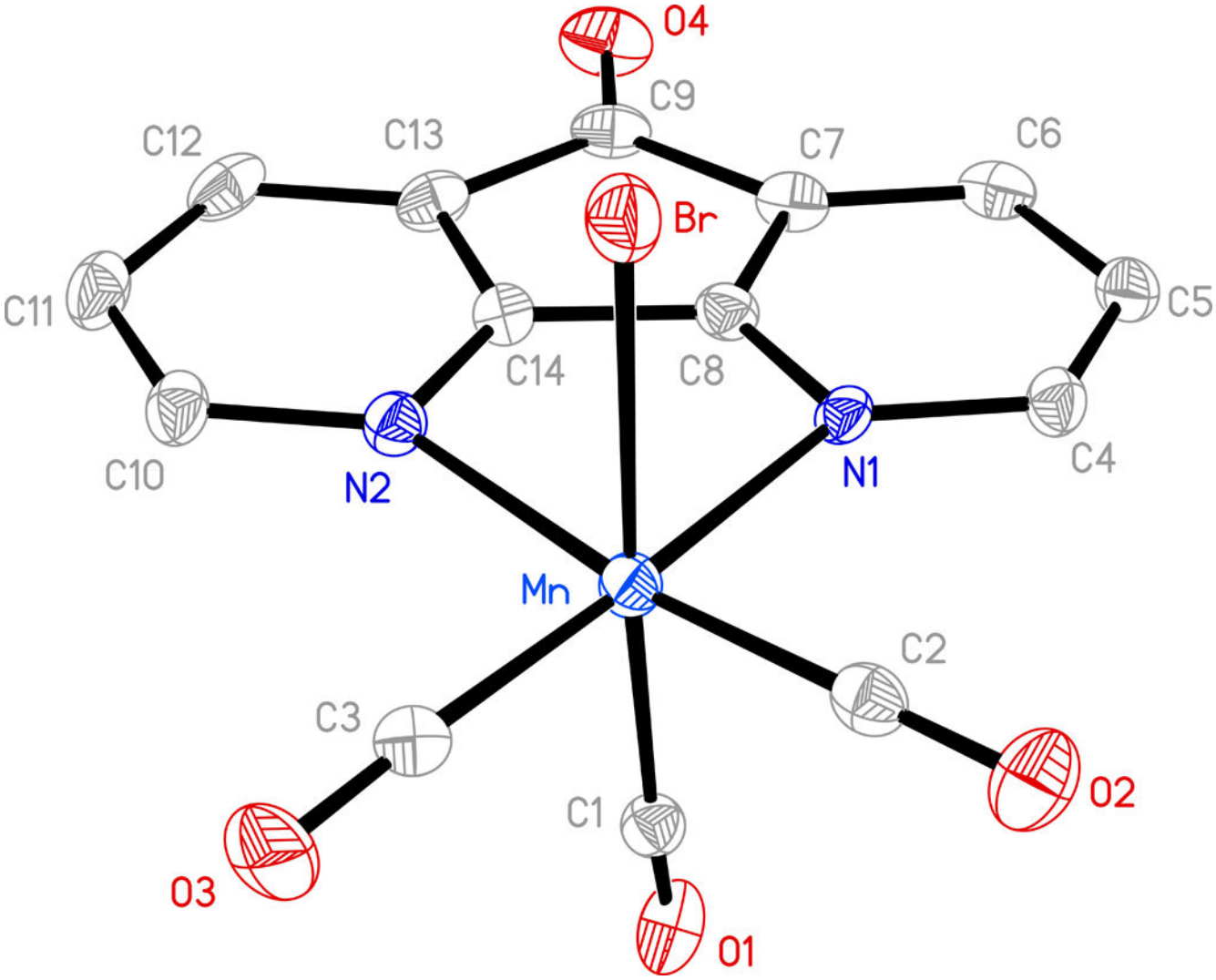

Figure 3.

Molecular structure of $[MnBr(CO)_3(dafo)]$ (**3**) (thermal ellipsoids are shown at 50% probability level and the hydrogen atoms are omitted for clarity) and selected bond distances (Å): Mn-C(1) 1.911(10), Mn-C(2) 1.794(9), Mn-C(3) 1.823(9), Mn-N(1) 2.103(6), Mn-N(2) 2.135(6), Mn-Br 2.5103(16).

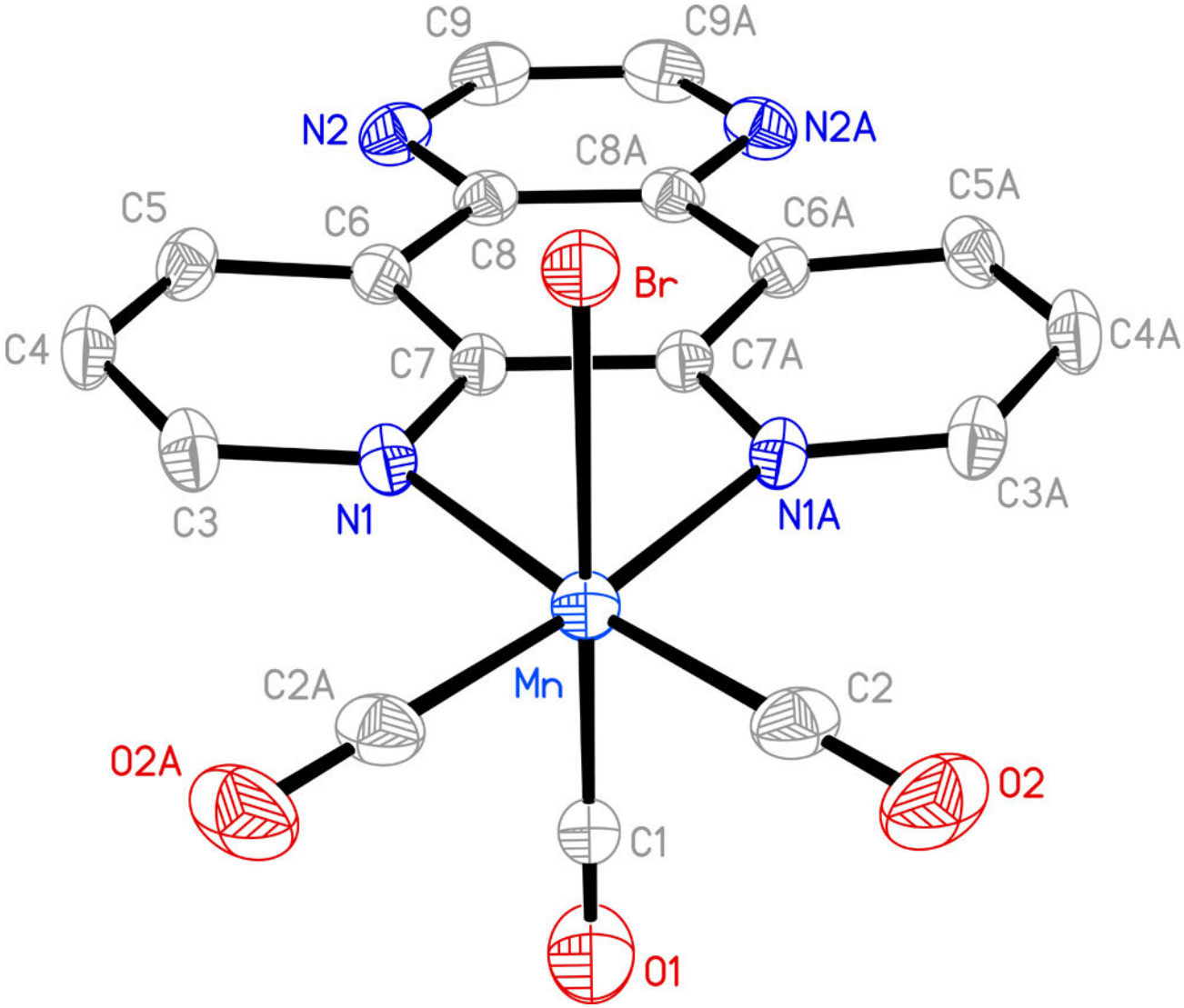

Figure 4.

Molecular structure of [$MnBr(CO)_3$(pyzphen)] (**4**) (thermal ellipsoids are shown at 50% probability level and the hydrogen atoms are omitted for clarity) and selected bond distances (Å): Mn-C(1) 1.867(6), Mn-C(2) 1.811(4), Mn-N(1) 2.055(2), Mn-Br 2.5290(8).

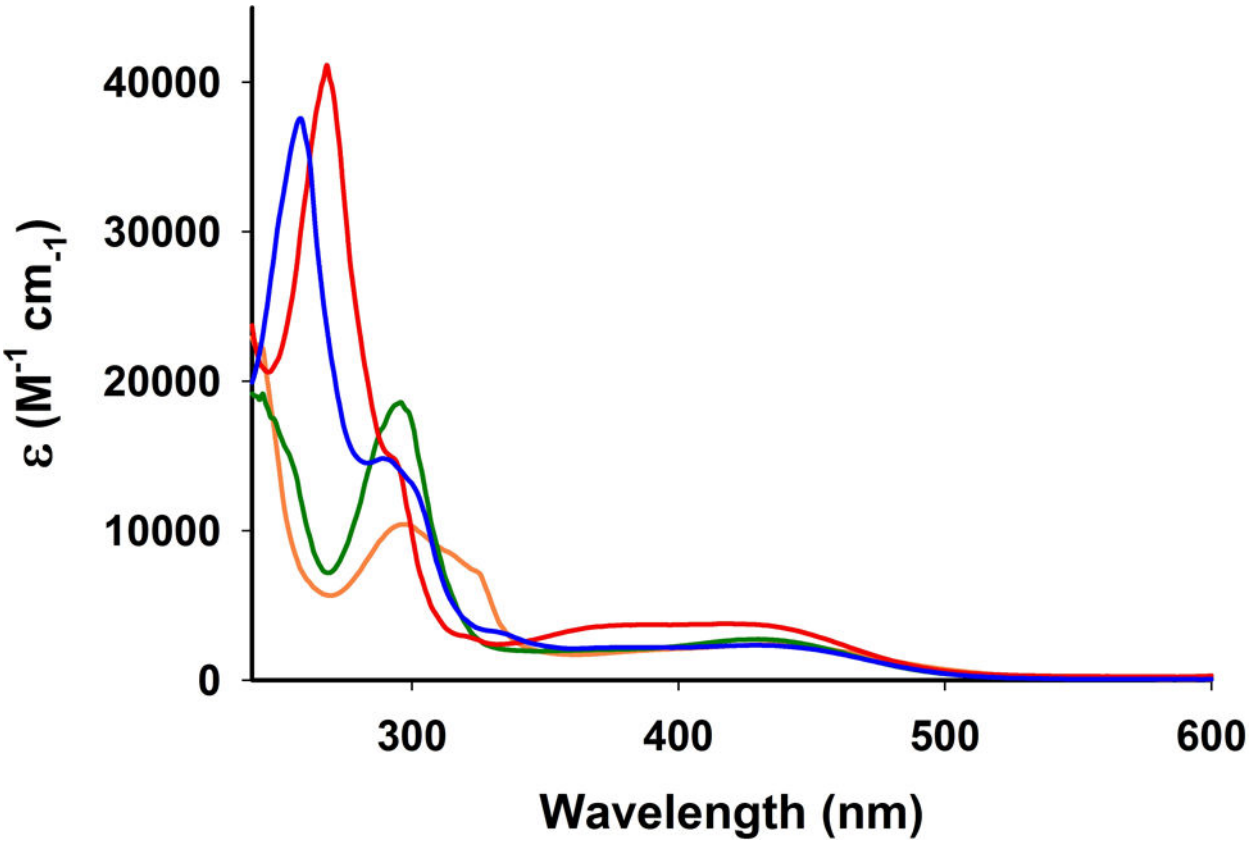

Figure 5.

Electronic absorption spectra of complex **1** (green), **2** (red trace), **3** (orange trace) and **4** (blue trace) in dichloromethane solution at 298 K

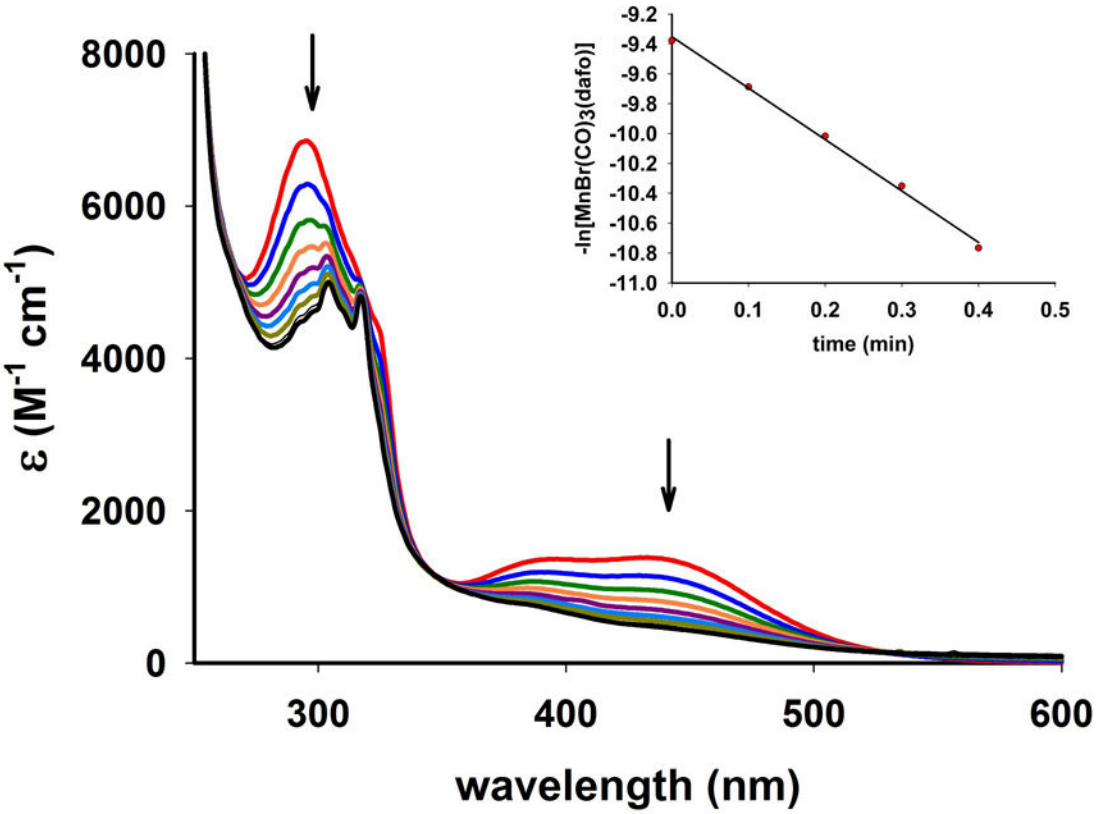

Figure 6.

Spectral changes in the electronic absorption spectrum of **3** in dichloromethane solution upon exposure to broadband visible light (power, 15 mW/cm^2). The inset displays the k_{CO} rate plot.

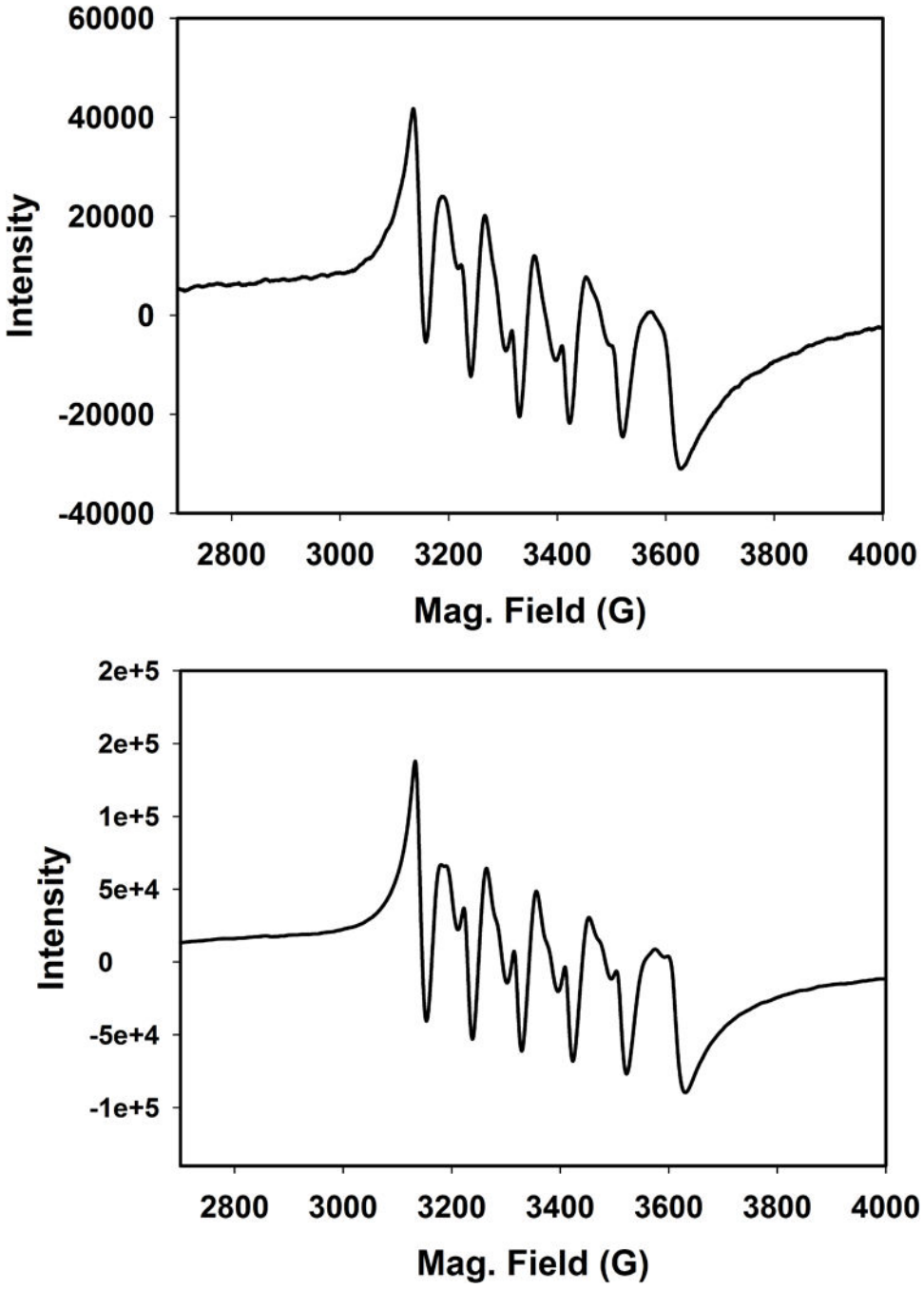

Figure 7.

X-band EPR spectrum (120 K) of the photolyzed solution of **2** (50 μM) in acetonitrile (top panel) and a reaction mixture of $Mn(ClO_4)_2$, 1,10-phenanthroline, and $(Et_4N)Br$ (1:1:1) in acetonitrile (bottom panel). Microwave frequency, 9.44 GHz; modulation amplitude, 2.00 G; modulation frequency, 100 kHz.

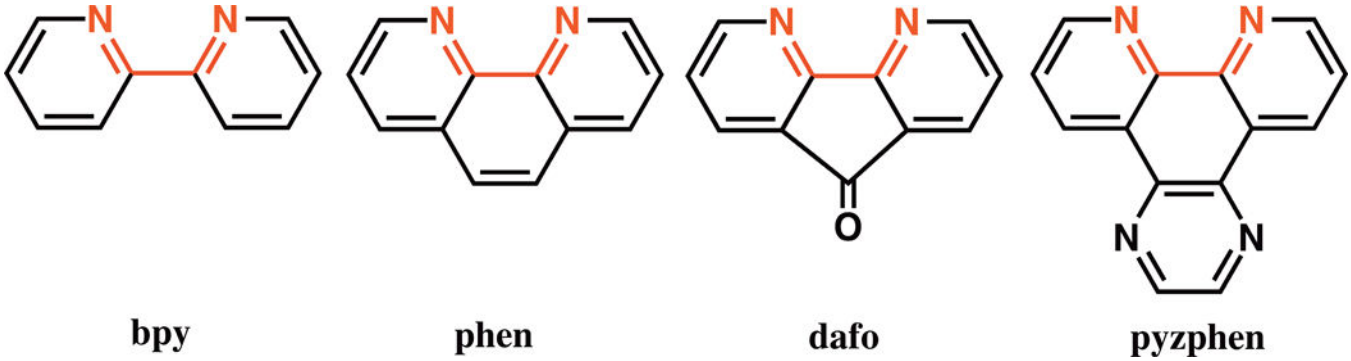

Scheme 1.

Rigid α-dimmime ligands employed for the synthesis of manganese carbonyl complexes described in this work

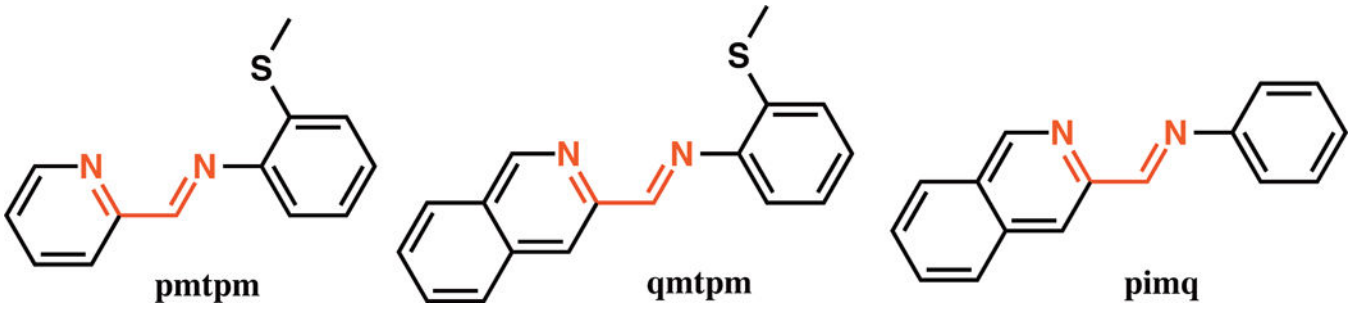

Scheme 2.
Non-rigid ligand frames with α-diimine functionality

Table 1

	1	**2**	**3**	**4**
Empirical formula	$C_{13}H_8BrN_2O_3Mn$	$C_{15}H_8BrN_2O_3Mn$	$C_{14}H_6BrN_2O_4Mn$	$C_{17}H_8BrN_4O_3Mn$
Formula weight	375.06	399.08	401.06	451.12
T(K)	296	296	296	296
λ (Å)	0.71073	0.71073	0.71073	0.71073
Crystal system	Triclinic	Monoclinic	Monoclinic	Monoclinic
Space group	P-1	I2/m	P2(1)/n	C2/m
a (Å)	11.034(5)	7.9775(6)	6.590(2)	15.6792(14)
b (Å)	11.084(5)	12.1132(9)	16.661(5)	11.2997(10)
c (Å)	11.679(5)	15.1968(10)	13.278(4)	9.2793(8)
α	85.295(5)	90	90	90
β (°)	85.749(5)	101.458(3)	100.983(4)	95.5910(10)
γ (°)	77.867(6)	90	90	90
V (Å^3)	1389.4(11)	1439.25(18)	1431.1(7)	1636.2(2)
Z	2	4	4	8
D_{calc} (Mg m^{-3})	1.793	1.842	1.861	1.831
Absorption Coeff (mm^{-1})	3.832	3.706	3.732	3.275
No. of unique reflections	4772	1204	2317	1366
Goodness-of-fit[a] on F^2	1.026	1.081	1.041	1.133
R_1[b]	0.0312	0.0240	0.0562	0.0287
wR_2[c]	0.0713	0.0660	0.1349	0.0755

[a] $GOF = [\Sigma[w(F_O^2-F_C^2)^2]/(N_O-N_V)]^{1/2}$ (N_O = number of observations, N_V = number of variables).

[b] $R1 = \Sigma||F_O|-|F_C||/\Sigma|F_O|$.

[c] $wR2 = [(\Sigma w(F_O^2-F_C^2)^2/\Sigma|F_O|^2)]^{1/2}$

Table 2

k_{CO} data for complexes **1**–**4** in dichloromethane solutions at 298 K

Complexes	Apparent CO release rate (k_{CO})[a] in min^{-1}	
	Visible light illumination	***UV light illumination***
1	1.21± 0.02 (1.15×10^{-4} M)	12.11± 0.03 (4.50×10^{-4} M)
2	4.65± 0.03 (2.25×10^{-4} M)	12.44± 0.03 (4.50×10^{-4} M)
3	3.44± 0.02 (4.50×10^{-4} M)	13.18± 0.02 (4.50×10^{-4} M)
4	6.29± 0.03 (2.67×10^{-4} M)	20.94± 0.03 (2.67×10^{-4} M)

[a]Concentrations are given within parenthesis

Table 3

Cyclic voltammetry data for complexes **1**–**4** in dichloromethane at 298K

Complexes	E_{pa} *a, b* (mV) (Mn^{I}/Mn^{II})
1	734
2	725
3	767
4	723

a $TBAPF_6$ (0.15 M) as supporting electrolyte.

b Scan rate, 100 mV/s